Supporting Information

Adsorption of Galloyl Catechin Aggregates Significantly Modulates Membrane Mechanics in Absence of Biochemical Cues

Takahisa Matsuzaki,[ab] Hiroaki Ito,[bc] Veronika Chevyreva,[b] Ali Makky,[bd] Stefan Kaufmann,[b] Kazuki Okano,[a] Naritaka Kobayashi,[e] Masami Suganuma,[e] Seiichiro Nakabayashi,[a] Hiroshi Y. Yoshikawa,[a] Motomu Tanaka[bf]**

[a.]Department of Chemistry, Saitama University, Sakura-ku, Saitama, 338-8570, Japan.

[b.]Physical Chemistry of Biosystems, Institute of Physical Chemistry, Heidelberg University, D69120 Heidelberg, Germany.

[c.]Department of Physics, Graduate School of Science, Kyoto University, Kyoto 606-8502, Japan.

[d.]Institut Galien Paris-Sud, CNRS, Univ. Paris-Sud, University Paris-Saclay, 92296 Châtenay-Malabry, France.

[e.]Graduate School of Science and Engineering, Saitama University, Shimo-okubo 255, Sakura-ku, Saitama 338-8570, Japan.

[f.]Institute for Integrated Cell-Material Sciences (WPI iCeMS), Kyoto University, 606-8501, Kyoto, Japan.

[*]Authors to whom correspondence should be addressed.

Electronic mail: hiroshi@mail.saitama-u.ac.jp Tel: +81-(0)-48-858-3379

Electronic mail: tanaka@uni-heidelberg.de Tel: +49-(0)-6221-544916 FAX: +49-(0)-6221-544918

1. Solubility enhancement of catechin powder

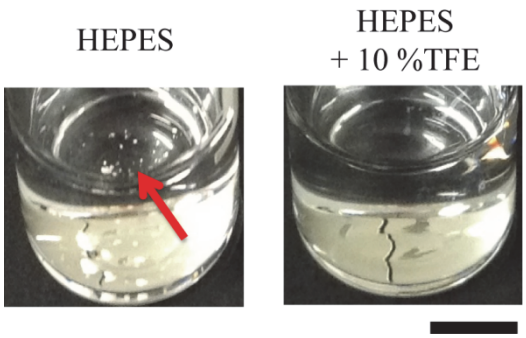

Figure S1. Glass vials filled with 6 mM EGCG solution without (left) and with (right) 10 % (v/v) trifluoroethanol (TFE). Red arrow shows the residue of EGCG powder. Scale bar is 0.5 mm.

2. Surface activity of catechin solution (without lipids)

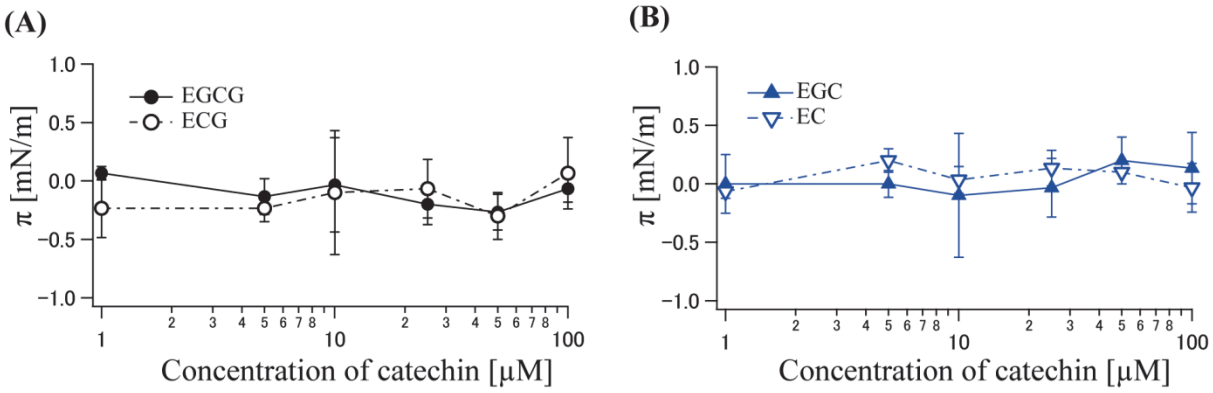

Figure S2. Surface activity of solutions of (A) EGCG and ECG (B) EGC and EC (without lipids). Surface pressure (π) of 300 μL catechin solutions was measured by a Micro trough X film balance (Kibron Inc., Espoo, Finland). Each data point corresponds to a mean value of three independent measurements. The error bar represents standard deviation.

3. Influence of TFE on surface pressure of monolayer (without catechin)

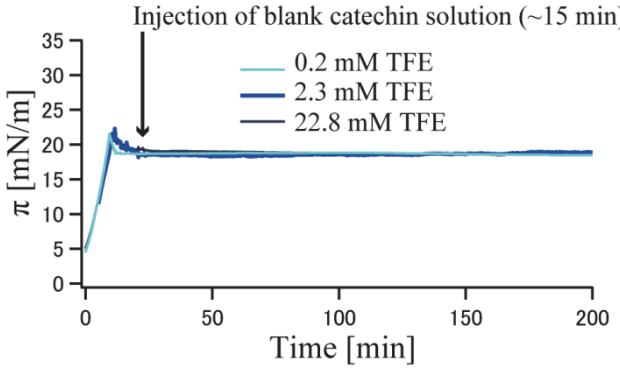

Figure S3. Time evolution of π of an OPPC monolayer after the injection of TFE solutions. Final concentration of TFE in the subphase is displayed.

4. Microscopic characterization of particle supported membranes

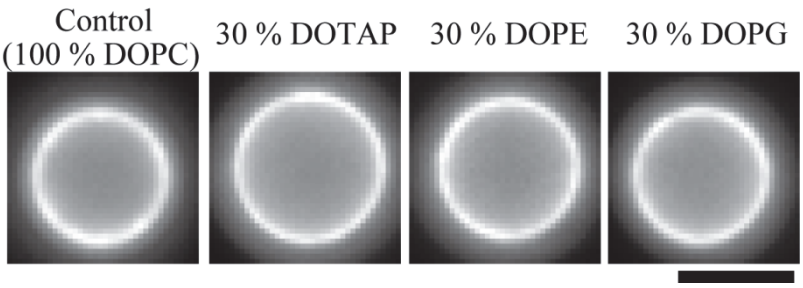

Figure S4: Fluorescence images of silica beads with differently charged lipids. For the epi-fluorescence observation, TRITC-DHPE (N-(6-tetramethylrhodamine-6-thiocarbamoyl)-1,2-dihexadecanoyl-sn-glycero-3-phosphoethanol amine, Molecular Probes, Paisley, UK) was doped into each lipid membranes. Final concentration of TRITC-DHPE in the lipid membrane was 0.2 mol %. Scale bar is 5 μm.

5. Organic solvent to disperse catechin aggregates

During the preparation, we examined several organic solvents to ensure that catechin molecules are dissolved. Figure S5 shows the results of fluorescence measurements of catechin derivatives in a HEPES buffer with or without an organic solvent. Catechin derivatives with iso-popanol or ethanol show significantly higher fluorescence intensity compared to those in aqueous buffers. This indicates that catechin aggregates via π-π interaction[1] were dissociated with the organic solvents.

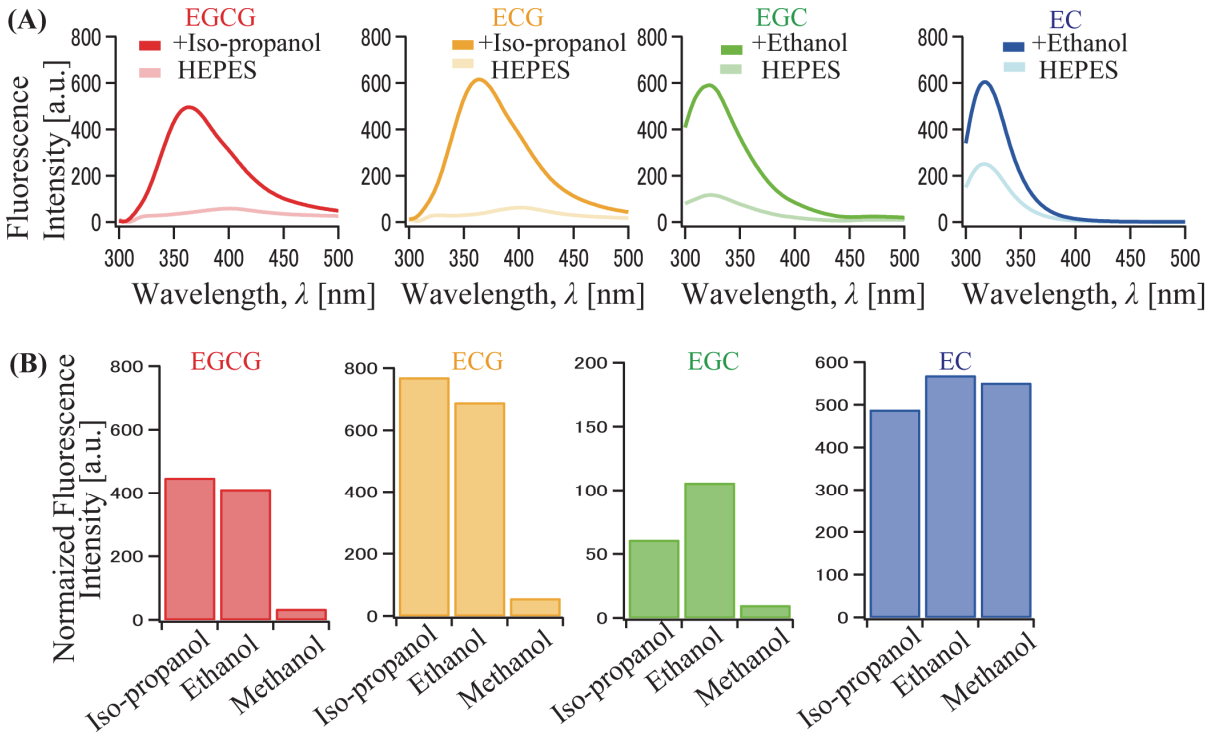

Figure S5: Evaluation of solubility of catechin derivatives in organic solvents (A) Representative fluorescence spectra of catechin derivatives (10 μM in final) in a pure HEPES buffer with or without an organic solvent (67 % v/v in final). Excitation wavelength was 280 nm. (B) Fluorescence peak intensity of each catechin derivative in an organic solvent normalized by that in a HEPES buffer.

6. Calibration curve for the determination of partition coefficient

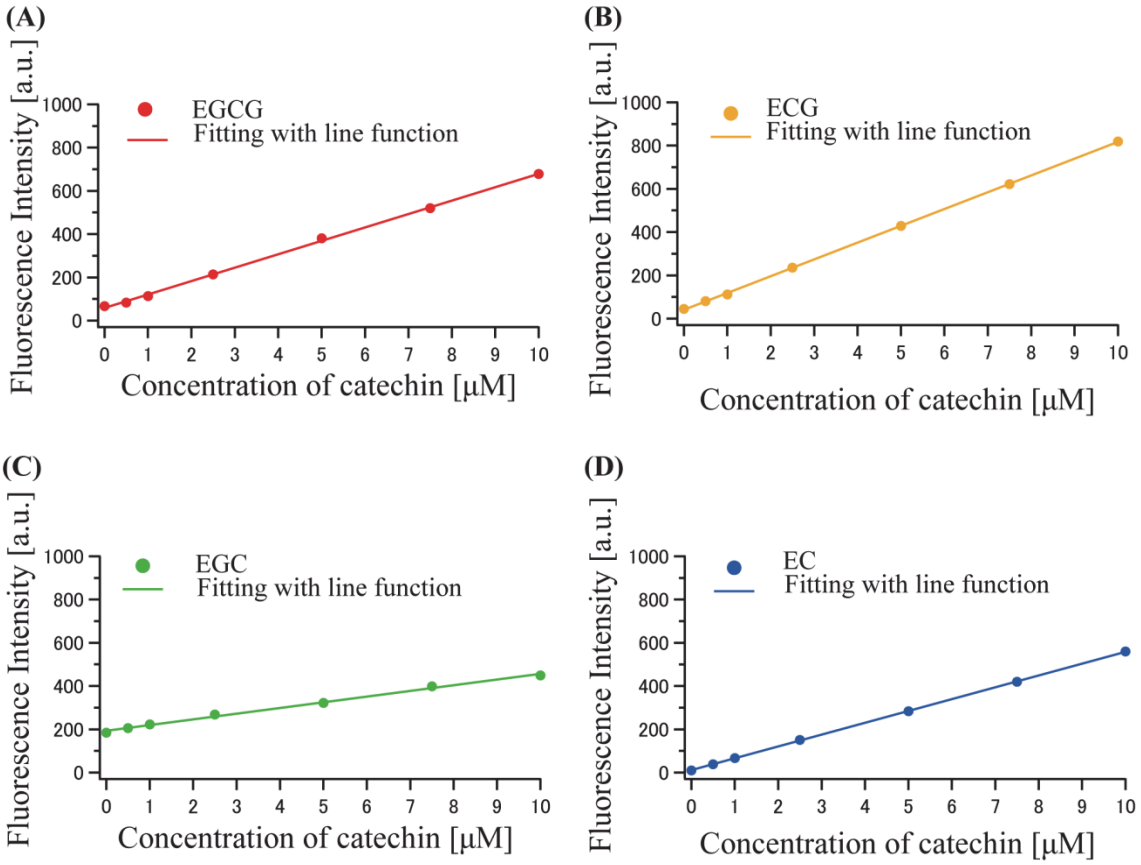

Figure S6. Calibration curve for the determination of partition coefficient. Excitation wavelength was 280 nm. Fluorescence spectra of each catechin derivatives showed a sharp peak at λ = 360 nm (EGCG), 361 nm (ECG), 332 nm (EGC), and 316 nm (EC), respectively. Solid lines represent the fitting with a line function.

7. Procedure to detect the edge of GUVs

First, the phase contrast images were processed by using a command of "gradient magnitude" of an Image J plugin "Image Differentials" (http://bigwww.epfl.ch/thevenaz/differentials/), written by Philippe Thévenaz, Biomedical Imaging Group, Swiss Federal Institute of Technology Lausanne.[2,3] The processed image showed a sharp peak at the boundary between GUV and halo, where the first derivative of the original intensity profile in a radial direction becomes extremum (Figure S7). Then, the peak position determined by fitting with Gaussian functions was defined as the position of GUV edge.

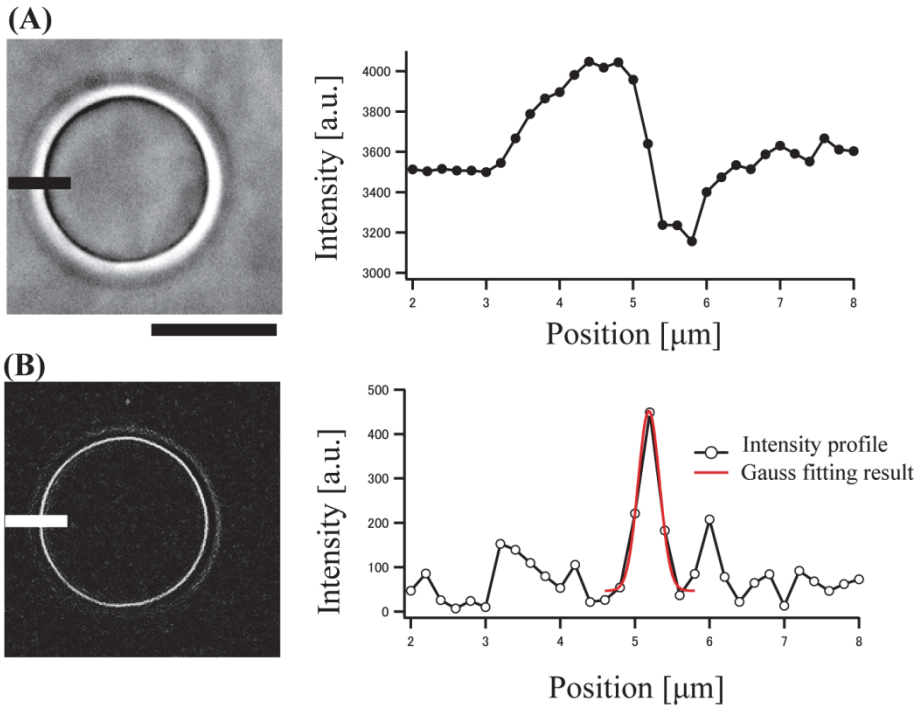

Figure S7. Phase contrast images of GUV (A) before and (B) after processing by Image differentials functions with corresponding line profiles taken along (A) the black line and (B) the white line in the images. Differential magnitude shows sharp peak and 5 points including peak was fitted with gauss function (red line). Scale bar is 10 μm. Osmolality of internal sucrose solutions of GUVs (~ 312 mOsm/kg) was adjusted to be slightly lower than that of outer glucose solutions (~ 356 mOsm/kg) to enhance the thermal fluctuation, thus edge detection was successful during the experiment.

8. Determination of bending stiffness (k_c) of GUV membrane

(A) Control (no catechin)

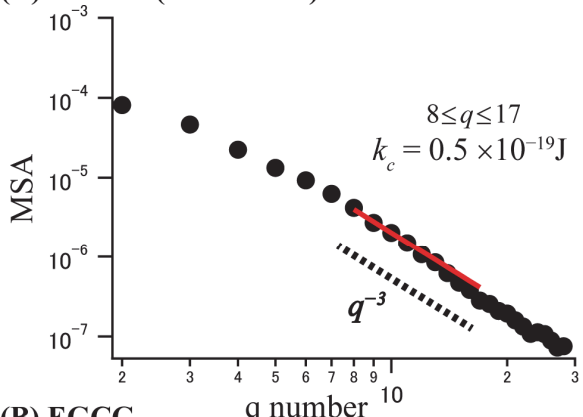

(B) EGCG

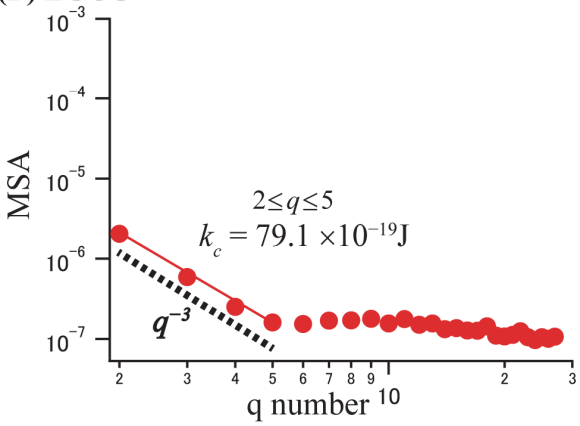

(C) ECG

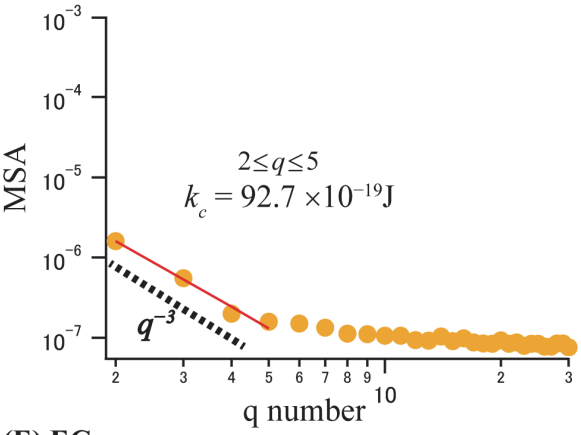

(D) EGC

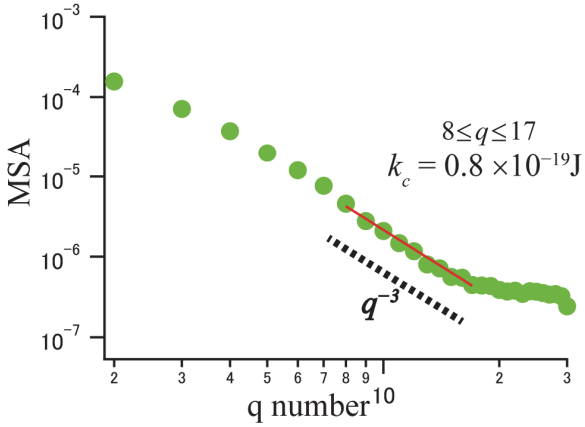

(E) EC

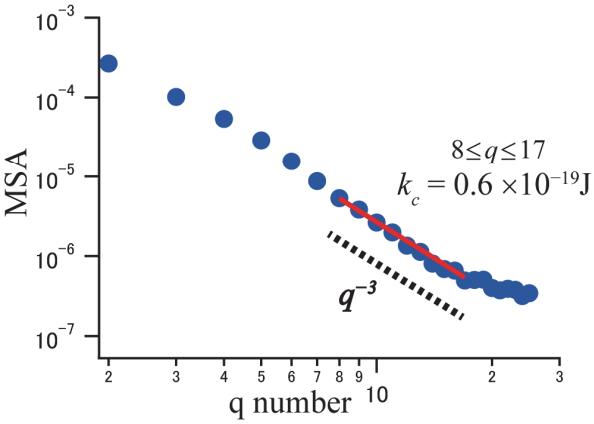

Figure S8. Representative mean squared amplitude (MSA) of GUV in the absence/presence 1 μM catechin derivatives. The red solid lines represent fitting lines with eq 4 (in the main text), and yield bending stiffness (k_c) of GUV membrane. Black dotted lines in (A)-(E) show q^{-3} power law (*i.e.,* bending dominated) regime.[4] It should be noted that MSA only follows q^{-1} (*i.e.,* tension-dominated) regime was not included in our MSA analysis. In addition, GUVs used for our analysis were single and isolated (supplementary movies) with a comparable size distribution (Figure S9).

9. Diameter of GUVs used for the flicker analysis

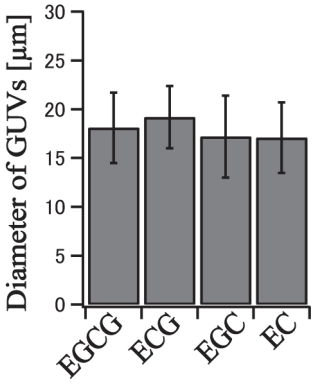

Figure S9 Diameter of GUVs used for the flicker analysis in Figure S8.

10Autocorrelation analysis

For a cross-check of the MSA analysis, which evaluates spatial information (amplitude and shape), we performed autocorrelation analysis (decay time). According to Duwe *et al.*, we calculated the autocorrelation given by[5]

$$A_q(\tau) = \frac{1}{S}\frac{1}{N-\tau}\sum_{n=1}^{N-\tau} v_q(t_n)v_q^*(t_{n+\tau}) \quad \text{(S1)}$$

where

$$S = \frac{1}{N}\sum_n \left|v_q(t_n)\right|^2$$

N is the number of frames, and n is an index of discretized time. v_q^* denotes the complex conjugate of v_q. On the other hand, the theoretical autocorrelation function is given by[6]

$$\left\langle v_q(t)v_q^*(0)\right\rangle = e^{-\omega_l t} \quad \text{(S2)}$$

where

$$\omega_l = \frac{k_c}{\eta R_0^3}\frac{l(l+1)}{(2l+1)(2l^2+2l-1)}(l+2)(l-1)\{l(l+1)+\sigma(\Delta)\} \quad \text{(S3)}$$

is the reciprocal characteristic decay time and η is the viscosity of aqueous solution. We here set $l = q$ as a good approximation, which has been conventionally used.[5] Fig. S10 shows the autocorrelation curves of the same vesicles used in Figure S8. The autocorrelation curves of control (no catechin), EGC, and EC can be well-fitted by a single exponential function with the characteristic decay time scale of seconds. We determined the bending stiffness by the least square fittings for $2 \leq q \leq 17$ and found that the obtained bending stiffness (e.g., $k_c \sim 1.0 \times 10^{-19}$ J for control) is comparable with those determined by the MSA analysis. On the other hand, the autocorrelation curves for EGCG and ECG show a sharp drop-off in the camera acquisition time (~ 60 ms), which can be attributed to the decay time of thermal fluctuation of membranes because the corresponding MSA is above noise level and in bending-dominated (q^{-3}) regime in small wavenumber modes. Using this longest possible decay time ($\omega_l^{-1} \sim 60$ ms) and parameters in eq. S3 ($\eta \sim 7 \times 10^{-4}$ Pa·s, $R_0 \sim 10^{-5}$ m, $\sigma \sim 0$, and $l \approx 2$), we can estimate the lowest limit of k_c (~ 5.3×10^{-18} J), which is about 50 times larger than that of control ($k_c \sim 1.0 \times 10^{-19}$ J). Thus this result of the autocorrelation analysis strongly supports our findings with the MSA analysis that k_c becomes significantly larger with EGCG and ECG.

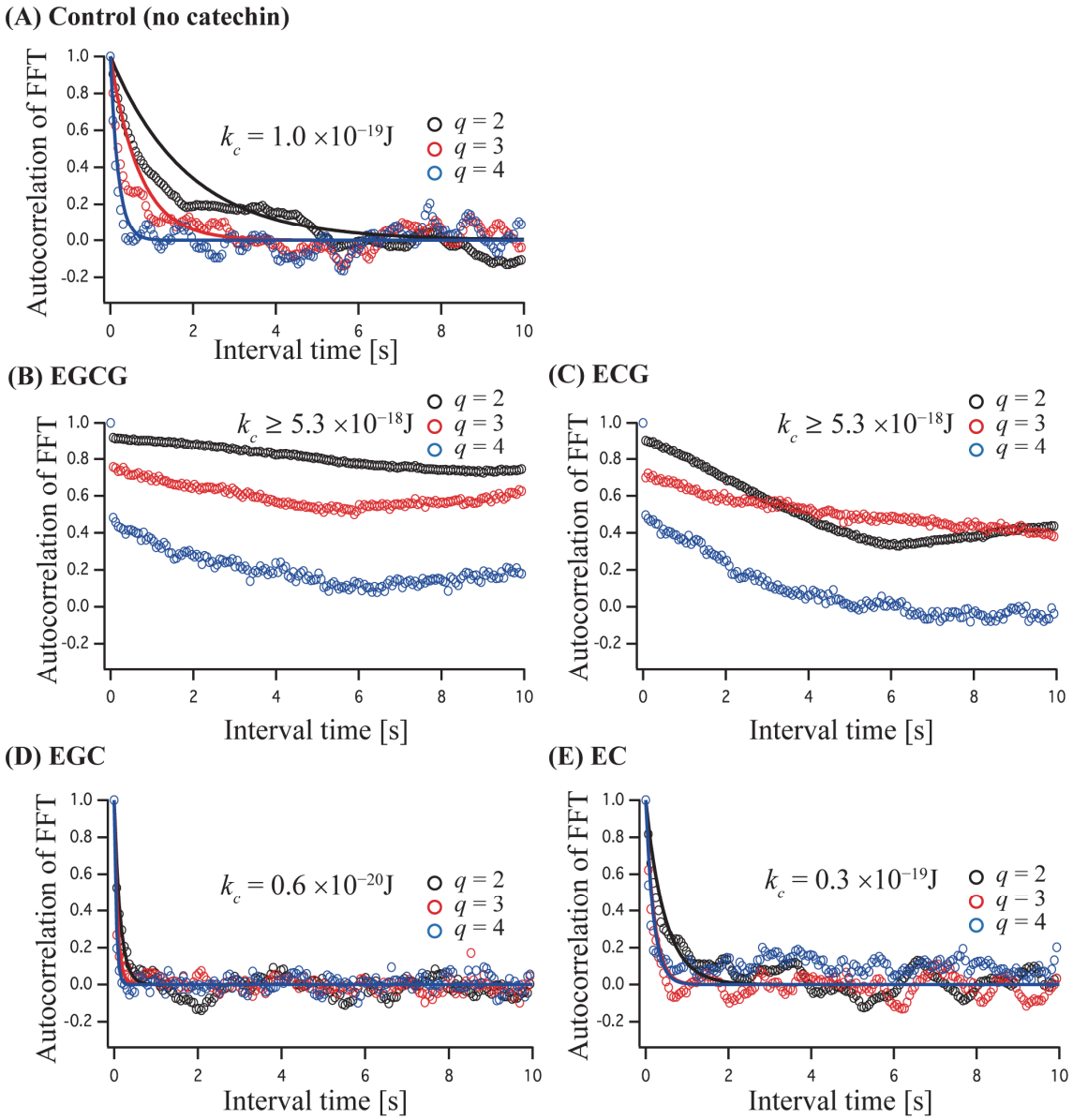

Figure S10. Representative autocorrelation (eq S1) of GUVs in the absence/presence of 1 μM catechin derivatives for wavenumber q = 2 (black), 3 (red), and 4 (blue). The same GUVs that were analyzed in Fig. S8 were used. The solid lines represent fitting lines (eq S2) and yield the decay time (ω_l) of (A) 1.9 s, (D) 0.43 s, (E) 0.46 s and the corresponding bending stiffness (k_c). Autocorrelation for (B) EGCG and (C) ECG exhibit a sudden drop-off in ~ 60 ms, indicating that GUV membranes become significantly stiffened with EGCG and ECG.

11. Fluorescence spectra of catechin derivatives with lipid vesicles

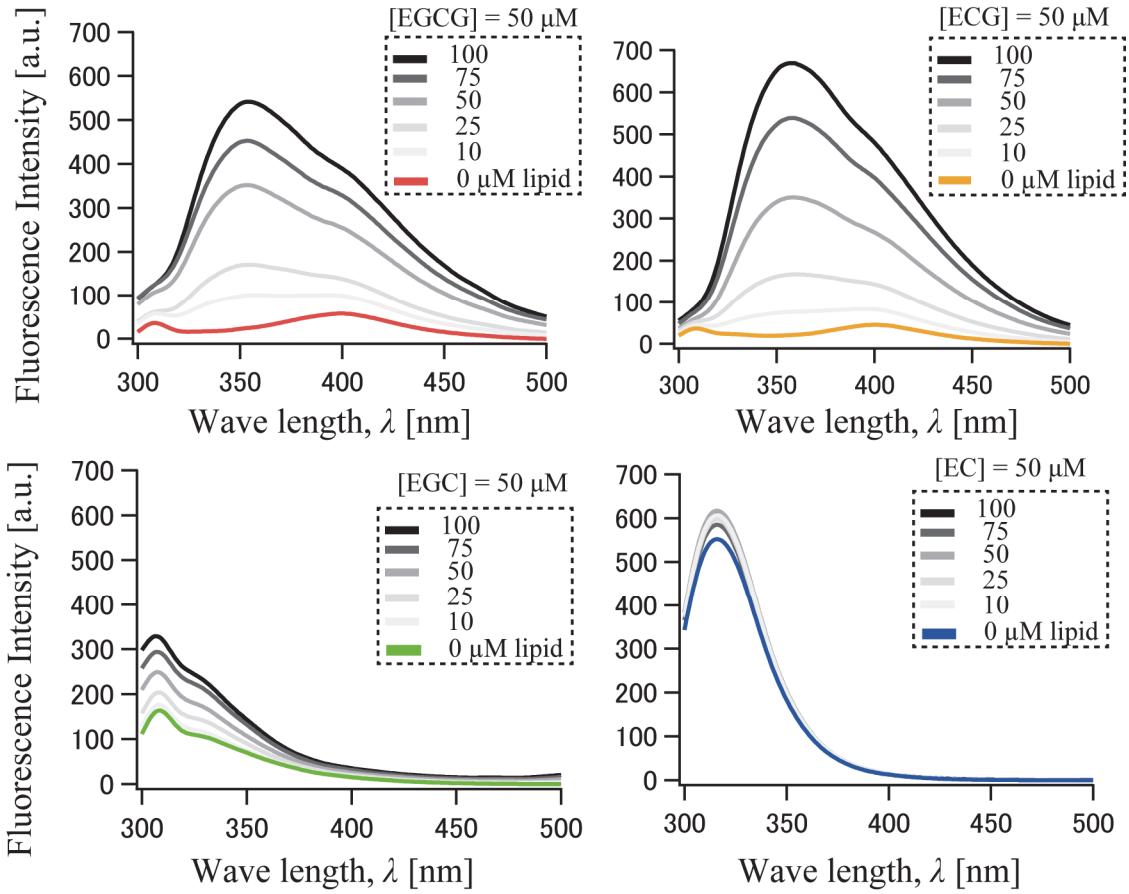

Figure S11. Fluorescence spectra of catechin derivatives (50 μM in final) with the different concentration of DOPC SUVs in HEPES buffer solutions.

12. Flickering GUV in the absence and presence of catechins

Supplementary movies are available as follows. It should be noted that we show a part of the movie for 3s in total (60 ms/flame) after JPG compression due to the file size limitation.

Supplementary_movie_1.avi: Flickering GUV in the absence of catechins (control)

Supplementary_movie_2.avi: Flickering GUV in the presence of 1 μM EGCG

Supplementary_movie_3.avi: Flickering GUV in the presence of 1 μM ECG

Supplementary_movie_4.avi: Flickering GUV in the presence of 1 μM EGC

Supplementary_movie_5.avi: Flickering GUV in the presence of 1 μM EC

REFERENCES

(1) Kitano, K.; Nam, K. Y.; Kimura, S.; Fujiki, H.; Imanishi, Y.; Sealing effects of (-)-epigallocatechin gallate on protein kinase C and protein phosphatase 2A. *Biophys. Chem.,* **1997**, *65*, 157-164.

(2) Unser M.; Splines: A Perfect Fit for Signal and Image Processing, *IEEE Signal Processing Magazine*, **1999**, *16*, 22-38.

(3) Thévenaz, P.; Blu, T.; Unser, M. Interpolation revisited. *IEEE Transactions on Medical Imaging*, **2000**, *19*, 739-758.

(4) Häckl, W.; Seifert, U.; Sackmann, E.; Effects of fully and partially solubilized amphiphiles on bilayer bending stiffness and temperature dependence of the effective tension of giant vesicles. *J. Phys. II France.* **1997**, 7, 1141-1157.

(5) Duwe, H. P; Kaes, J.; Sackmann, E. Bending elastic moduli of lipid bilayers: modulation by solutes. *J. Phys. France.* **1990**, 51, 945-962.

(6) Seifert, U. Configurations of fluid membranes and vesicles. *Adv. Phys.* **1997**, 46, 13-137.